Polymer 51 (2010) 3918–3925

Contents lists available at ScienceDirect

Polymer

journal homepage: www.elsevier.com/locate/polymer

Rheological modelling of the free-radical crosslinking of PDMS rubber in the presence of TEMPO nitroxide

Skander Mani [a,b,c,d], Philippe Cassagnau [b,c,d,*], Mosto Bousmina [e], Philippe Chaumont [b,c,d]

[a] Department of Chemical Engineering, Laval University, Quebec G1V 0A6, Canada
[b] Université de Lyon, F-69003, France
[c] Université de Lyon 1, F-69622, CNRS UMR5223, France
[d] Ingénierie des Matériaux Polymères: Laboratoire des Matériaux Polymères et Biomatériaux, 15 Boulevard Latarjet, F-69622 Villeurbanne, France
[e] Institute for Nanomaterials and Nanotechnology (INANOTECH), Hassan II Academy of Science and Technology, Rabat, Morocco

ARTICLE INFO

Article history:
Received 16 April 2010
Received in revised form
13 June 2010
Accepted 14 June 2010
Available online 22 June 2010

Keywords:
Viscoelasticity
Crosslinking
PDMS

ABSTRACT

The aim of the present work is to study the free-radical kinetics of PDMS rubber crosslinking in the presence of 2,2,6,6-tetramethylpiperidinyloxyl (TEMPO) nitroxide. For this purpose a new method based on the relationship between the kinetics of the macro-radicals coupling [$R_{cc}(t)$] was derived from a fundamental kinetic model and the viscoelastic changes of the complex shear modulus ($G'(t)_\omega$ and $G''(t)_\omega$). The kinetic model takes into account the initiator (Dicumyl peroxide in the present study) decomposition and the trapped PDMS macro-radicals in the presence of a radical scavenger such as TEMPO. Activation energy E_{ac} and collision frequency factor A_{0c} for the bimolecular termination reaction coefficient rate k_{cc} have been derived from the anisothermal DSC results according to the Kissinger method. Furthermore, it was observed that addition of TEMPO nitroxide can boost the initiator efficiency. The concentration variation of the active PDMS carbon-centred radicals $[R_p^{\bullet}(t)]_{act}$ and the $[R_{cc}(t)]$ with reaction time were predicted using this kinetic model. On the other hand, the influence of TEMPO concentration in formulation ($[N]_0$) and effect of temperature on viscoelastic variations are studied. As a main result, the rheological modelling shows that this new method accurately predicts the time variation of complex shear modulus at any temperature and [TEMPO]/[DCP] ratio.

1. Introduction

Modelling of crosslinking process has recently received a great deal of attention [1]. Actually, modelling of the variation of the viscoelastic properties during crosslinking is of particular importance from a processing point of view. This modelling requires in-depth study of chemistry of reaction, kinetic models [2], molecular structure, and changes in mechanical properties during crosslinking process [3]. However, free-radical crosslinking of rubber is a very complex chemical process and no known simulation techniques can directly investigate the changes in physico-chemical properties of the crosslinked network at molecular scale.

Commonly, a major curing mechanism frequently used for elastomers is the generation of polymer radicals (through the use of organic peroxides) that subsequently combine to form carbon–carbon bonds [4]. However, free-radical crosslinking by organic peroxide suffers from premature crosslinking at high temperatures, which is called scorching [5]. Chaudhary et al. [6] showed that the reaction of carbon-centred radicals with nitroxides and its derivatives can be a novel mean for scorch suppression, cure control and functionalisation in peroxide crosslinking of polyethylene thermoplastic. On the other hand, we investigated in a previous work [7] the effect of TEMPO in free-radical mechanism of vinyl-PDMS rubber crosslinking initiated by dicumyl peroxide (DCP) and noted a remarkable scorch delay by varying the molar ratio [TEMPO]/[DCP] in the range $r = 0$ to 2.4. Furthermore, the characterisation of the network features based on the phenomenological model of Langley [8] and Dossin and Graessley [9] demonstrated that the control of the network topology can be achieved by using TEMPO nitroxide. Nitroxide chemistry has opened a new avenue in the domain of radical chemistry development for polymers. For example, Robert [10] patented a process for grafting maleic anhydride onto a thermoplastic polymer in the presence of a nitroxide such as TEMPO to avoid crosslinking during the grafting operation. More recently, Esseghir et al. [11] patented a new method of selecting a nitroxide for use as an inhibitor for free-radical crosslinking of EPDM elastomer.

* Corresponding author. Ingénierie des Matériaux Polymères: Laboratoire des *Matériaux Polymères* et Biomatériaux, 15 Boulevard Latarjet, F-69622 Villeurbanne, France. Tel.: +33 4 72446208; fax: +33 4 72431249.
E-mail address: philippe.cassagnau@univ-lyon1.fr (P. Cassagnau).

0032-3861/$ – see front matter © 2010 Elsevier Ltd. All rights reserved.
doi:10.1016/j.polymer.2010.06.029

The aim of the present work is to introduce a new simple modelling technique for direct investigation of the variations in viscoelastic properties during randomly crosslinking process in the presence of TEMPO. This modelling aims to predict the variation of complex shear modulus ($G'(t)_\omega$ and $G''(t)_\omega$) from the kinetics of macro-radicals coupling. The present study is based on free-radical crosslinking of PDMS used as a model system as described in our previous work [7]. Actually, the presence of vinyl functional groups in the polymer chain enables the free-radical crosslinking of PDMS [12] with control over crosslink structure.

2. Experimental procedures

2.1. Differential scanning calorimetry (DSC)

Differential scanning calorimeter equipment manufactured by TA Instruments (Q100 system), equipped with Sealed aluminium pans, was used to measure the heat of crosslinking reactions. The mass of the samples ranged from 20 to 23 mg. A sealed empty pan was used as a reference. The total heats of reactions were obtained from non-isothermal method (Heating rate: $\dot{T} = 2.5,\ 5, 10,\ 15$ and 20 °C/min^{-1}). All experiments were performed under nitrogen purge.

2.2. Rheological measurements

The rheological experiments were carried out on a rheometrics mechanical spectrometer (RMS800) using a parallel-plate geometry ($R = 12.5$ mm). The parallel-plate system was preheated at the temperature of the experiment. Then, the sample was put between the plates once the temperature of regulation was reached. The rheological kinetics of crosslinking were measured in real time at only one pulsation ($\omega = 1$ rad s^{-1}) and at different temperatures $T = 160$, 180 and 200 °C. At the end of this crosslinking process, a frequency sweep experiment ($10^{-2} < \omega$ rad s$^{-1} < 10^2$) was performed on the same sample at the same temperature to determine the equilibrium modulus ($G_e = \lim_{\omega \to 0} G'(\omega)$).

Dynamic measurements during the non-isothermal conditions (Heating rate: $\dot{T} = 2.5,\ 5, 10,\ 15$ and 20 °C/min^{-1}) were used to compare with the DSC kinetics results. In all experiments, sample response linearity with respect to strain amplitude was verified, and nitrogen gas was used to prevent thermal oxidation. In this type of experiment, we assumed that DCP and TEMPO were perfectly dispersed in molten polymer at a molecular scale (homogeneous conditions of reaction).

3. Kinetic modelling

3.1. Mechanism assumptions

Free-radical crosslinking is a process of chemically producing network by creation of carbon to carbon crosslinking bond between polymer chains. PDMS that contain vinyl groups can be crosslinking by dialkyl peroxides such as dicumyl peroxide. The different steps of this chemical mechanism are shown in Fig. 1. The initiation step in peroxide-induced crosslinking is the thermal decomposition of the initiator to give two cumyloxyl free-radicals (reaction (1)). In the case of vinyl-PDMS, the radical addition predominates over abstraction route [13]. Therefore, next step is the addition of cumyloxyl radicals to a double bond of the polymer molecule (reaction (2)). The polymer radicals hence produced are quite reactive, so they combine to other polymer radicals to form a covalent carbon–carbon crosslinks (reaction (4)) [4]. Nevertheless, we revealed in our last study [7] that in the presence of inhibitor molecule like TEMPO nitroxide, the polymer radicals are

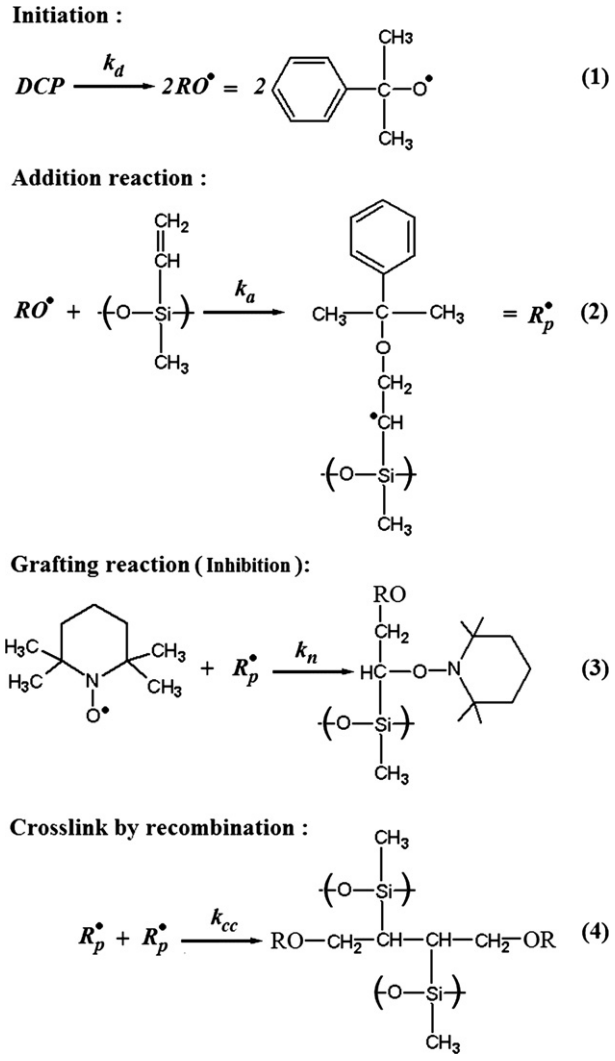

Fig. 1. Controlled free-radical crosslinking mechanism of vinyl-PDMS used in this simulation.

rapidly trapped by a grafting reaction before they are able to form crosslink. As shown in reaction (3), primary and secondary alkoxyamines (–C–O–N–) was formed between the nitroxyl and carbon-centred radicals (inactive PDMS macro-radical).

From a modelling point of view, several assumptions are necessary to reduce the number of parameters in the kinetic modelling of this complex crosslinking process:

1. The peroxide and nitroxide molecules are homogeneously distributed in the polymer. Furthermore, the reactions are not diffusion controlled [14]; so, the reaction rates for DCP decomposition and PDMS crosslinking were assumed constant during the course of reaction.
2. All cumyloxyl free-radicals produced from DCP decomposition have the same dissociation energy.
3. The reactivity of cumyloxyl free-radicals on the vinyl function of the PDMS is supposed to be constant.
4. The side reactions [7] coming from DCP molecules decomposition are negligible,
5. Inhibition involving primary radicals is negligible; i.e. TEMPO is capable of reacting and destroying only PDMS carbon-centred radicals,
6. Side reactions in the presence of TEMPO nitroxide, such as degradation of PDMS [7] are negligible.

According to these assumptions, the experimental results are then analysed by the simplified reactions scheme as described in Fig. 1.

3.2. Kinetic equations

According to Fig. 1, the initiation step may include the formation of initiated radicals and its reaction with pendent vinyl groups. Where $RO^{\bullet}$ represents the cumyloxyl radicals (primary radicals) and k_d is the coefficient rate for the initiator decomposition, which governs the previous process. The factor 2 refers to the formation of two free-radicals for each decomposed molecule of initiator. For the first order kinetics, the rate of initiator decomposition can be expressed as [15]:

$$\frac{d[DCP]}{dt} = -k_d[DCP(t)] \tag{1}$$

Where k_d can be simply derived from an empirical Arrhenius law:

$$k_d = A_0 \exp(-E_a/RT) \tag{2}$$

Where A_0 represents the collision frequency factor and E_a is the activation energy for the initiator decomposition reaction, with: $A_0 = 7.47 \times 10^{15}\ s^{-1}$ and $E_a = 153.5\ kJ\ mol^{-1}$ for DCP [16].

Reordering the above equation and integrating between the time at which the initiator is added $t = 0$ and the testing time t; we obtain:

$$[DCP(t)] = [DCP]_0 \exp(-k_d t) \tag{3}$$

Where $[DCP]_0$ is the initial concentration of DCP at $t = 0$. In the present study, $[DCP]_0 = 36 \times 10^{-3}\ mol\ L^{-1}$. $[DCP(t)]$ represents the residual concentration of the initiator at a reaction time t.

The coefficient rate of reaction (2), k_a, is in the range of 10^6 to 10^7 $L\ mol^{-1}\ s^{-1}$ [17] which is high enough as compared with k_d ($2.3 \times 10^{-3}\ s^{-1}$ at $T = 160\ ^{\circ}C$); so it can be supposed that the primary radicals produced in reaction (1) at a time t can be transformed immediately and completely into PDMS carbon-centred radicals in reaction (2). Moreover, in the presence of inhibitor like TEMPO, we showed [7], that the polymeric radicals are rapidly trapped by a grafting reaction before they are able to form crosslinks. Assuming that TEMPO is an efficient radical scavenger, i.e. TEMPO is capable of reacting with polymer macro-radicals only; its decomposition rate can be expressed as following:

$$\frac{d[N]}{dt} = -k_n \left[R_p^{\bullet}(t)\right]_{act}[N(t)] \tag{4}$$

Where $[N(t)]$ is TEMPO concentration, k_n is the coefficient rate of reaction (3), $[R_p^{\bullet}(t)]_{act}$ is active PDMS carbon-centred radicals' concentration and k_n is the coefficient rate of side reaction between the primary initiator radicals and TEMPO.

In addition, assuming bimolecular combination of backbone radicals [18], the rate of chain recombination (or crosslinking rate) described by reaction (4) is calculated according to the following equation:

$$\frac{d\left[R_p^{\bullet}(t)\right]_{act}}{dt} = 2\frac{d[R_{cc}(t)]}{dt} = -k_{cc}\left[R_p^{\bullet}(t)\right]_{act}^2 \tag{5}$$

Where k_{cc} is the rate of the disappearance of active PDMS macro-radicals by bimolecular termination and $[R_{cc}(t)]$ is the concentration of crosslink covalent bonds.

According to the crosslinking mechanism in Fig. 1, the increases rate of active PDMS macro-radicals in the presence of TEMPO can be expressed as:

$$\frac{d\left[R_p^{\bullet}(t)\right]_{act}}{dt} = 2f\,k_d[DCP(t)] - k_n\left[R_p^{\bullet}(t)\right]_{act}[N(t)] - k_{cc}\left[R_p^{\bullet}(t)\right]_{act}^2 \tag{6}$$

The parameter f in Eq. (6) is called the efficiency of initiator [19].

Moreover, we assumed that during scorch phase the bimolecular termination of PDMS macro-radicals is totally quenched ($k_{cc}([R_p^{\bullet}(t)]_{act})^2 = 0$), so $[R_p^{\bullet}(t)]_{act}$ and constant; and therefore quasi-steady-state approximation (QSSA) [20] is applied to Eq. (6) ($d[R_p^{\bullet}(t)]_{act}/dt = 0$):

$$\frac{d[N]}{dt} = -k_n\left[R_p^{\bullet}(t)\right]_{act}[N(t)] = -2fk_d[DCP(t)] \tag{7}$$

By substituting Eq. (3) into Eq. (7), it can be shown that the rate of inhibitor consumption is independent of the time variation of its concentration:

$$\frac{d[N]}{dt} = -2fk_d[DCP]_0\exp(-k_d t) \tag{8}$$

By integrating Eq. (8) with the initial conditions ($[N(t = 0)] = s \times [N]_0$); the nitroxide concentration obeys the following equation:

$$[N(t)] = (s \times [N]_0) - 2f[DCP]_0[1 - \exp(-k_d t)] \tag{9}$$

The parameter s in Eq. (9) is called the efficiency of nitroxide (TEMPO). It is defined as:

$$s = \frac{[C{-}O{-}N]_{formed}}{[N]_0} \tag{10}$$

Therefore, we can define scorch time (t_r) as the time at witch $[N(t = t_r)] = 0$. Accordingly and using Eq. (9), we obtain:

$$t_r = -\frac{1}{k_d}\ln\left[1 - \frac{[N]_0}{2\alpha[DCP]_0}\right] \tag{11}$$

With ($\alpha = f/s$) is the initiator and inhibitor efficiency ratio. After depletion of the inhibitor ($[N(t \geq t_r)] = 0$), active PDMS macro-radicals can combine and the crosslinking reaction occurs. Under such conditions and according to Eq. (6), $[R_p^{\bullet}(t)]_{act}$ increases at a rate of:

$$\frac{d\left[R_p^{\bullet}(t)\right]_{act}}{dt} = 2fk_d[DCP(t)] - k_{cc}\left[R_p^{\bullet}(t)\right]_{act}^2 \tag{12}$$

After initiation, the active macro-radicals concentration decreases according to the termination rate law (Eq. (5)). According to Eq. (12), the rate of active radical is not constant over the crosslinking process. Consequently, the steady-state principle does not hold true ($d[R_p^{\bullet}(t)]_{act}/dt \neq 0$). In order to find the time-dependent concentration $[R_p^{\bullet}(t)]_{act}$, the non-linear differential Eq. (12) was integrated with the initial value of $[R_p^{\bullet}(t = t_r)]_{act} = 0$ to finally obtain for $t \geq t_r$:

$$\left[R_p^{\bullet}(t)\right]_{act} = \left\{\left[\frac{2fk_d[DCP(t)]}{k_{cc}}\right]^{1/2} \times \tanh\left[(2fk_{cc}k_d[DCP(t)])^{1/2}(t - t_r)\right]\right\} \tag{13}$$

Following this and by substituting Eq. (3) into Eq. (13), the general kinetic law for $[R_p^{\bullet}(t)]_{act}$ is then derived:

$$\left[R_p^{\bullet}(t)\right]_{act} = \left\{\left[\frac{2fk_d[DCP]_0\exp(-k_d t)}{k_{cc}}\right]^{1/2} \times \tanh\left[(2fk_{cc}k_d[DCP]_0\exp(-k_d t))^{1/2}(t - t_r)\right]\right\} \tag{14}$$

Finally, using the mass conservation, the concentration of chemical bonds $[R_{cc}(t)]$ is determined as:

$$[R_{cc}(t)] = 1/2\left(\left[R_p^{\bullet}(t)\right]_{tot} - \left[R_p^{\bullet}(t)\right]_{act}\right) \quad (15)$$

With $[R_p^{\bullet}(t)]_{tot}$ is the concentration of the total macro-radicals generated without taking account the competition between initiation and chains recombination reactions. Integrating Eq. (12) between t_r and t with $k_{cc}([R_p^{\bullet}(t)]_{act})^2 = 0$ gives:

$$\left[R_p^{\bullet}(t)\right]_{tot} = 2f[DCP]_0(\exp(-k_d t_r) - \exp(-k_d t)) \quad (16)$$

By substituting Eq. (16) and (14) into Eq. (15), the kinetic model for this controlled crosslinking reaction and hence for the network growth prediction at the molecular scale can be expressed as following:

$$[R_{cc}(t)] = \left\{ \left[2f[DCP]_0(\exp(-k_d t_r) - \exp(-k_d t))\right] - \left[\frac{2fk_d[DCP]_0\exp(-k_d t)}{k_{cc}}\right]^{1/2} \times \tanh\left[\left(2fk_{cc}k_d[DCP]_0\exp(-k_d t)\right)^{1/2}(t - t_r)\right]\right\} \quad (17)$$

4. Results and discussion

4.1. Effect of TEMPO on the initiator efficiency

The scorch time (t_r) is also defined as the time at which the active polymer macro-radicals suddenly increase. From a viscoelastic point of view, the scorch time is defined [7] as the time at which the storage modulus suddenly increases (See ahead in Fig. 9). The Eq. (11) was derived from the assumption that the efficiency f of initiator is constant, regardless of the other crosslinking conditions. However, f can be affected by the crosslinking conditions such as temperature, crosslinking density and concentration of initiator and/or inhibitor [21]. Reordering Eq. (11), we express the variation of the initiator and inhibitor efficiency ratio ($\alpha = f/s$) vs $[N]_0$ and $[DCP]_0$:

$$\alpha = \frac{[N]_0}{2[DCP]_0[1 - \exp(-k_d t_r)]} \quad (18)$$

Fig. 2a shows the dependence of α on $[N]_0$ from the experimental variation of t_r at $T = 160\ ^{\circ}C$. The results shown in Fig. 2a prove that α is not constant but linear-dependent on the amount of TEMPO. Consequently, the linear extrapolation of the values obtained for $r =$ 1.2, 1.6, 1.8 and 2 (see Table 1) allows us to determine the dependence of α on the initial concentration of TEMPO:

$$\alpha = c_1 \times [N]_0 + \alpha_0 \quad (19)$$

Where, $\alpha_0 = 0.69$ and $c_1 = 5.2$ (mol^{-1} L).

According to Eq. (19) and initial conditions ($[DCP]_0 = 36 \times 10^{-3}$ mol L^{-1} and $f_0 = 0.31$ [7] for $r = 0$ (TEMPO free)), the inhibitor efficiency s must be equal to 0.45. Subsequently, from Eq. (19) and with the calculated value for s, the dependence of f on the initial concentration of TEMPO can be predicted by the following equation:

$$f = c_2 \times [N]_0 + f_0 \quad (20)$$

Where, $f_0 = 0.31$ and $c_2 = 2.34$ mol^{-1} L.

As a result, Fig. 2a shows that initiator efficiency increases from 0.31 to 0.485 with $[N]_0$ (TEMPO concentration, see Table 1). This result is in agreement with the experiment results of Zhang and Ray [22]. Indeed, these authors proved that addition of stable radicals can boost the initiator efficiency.

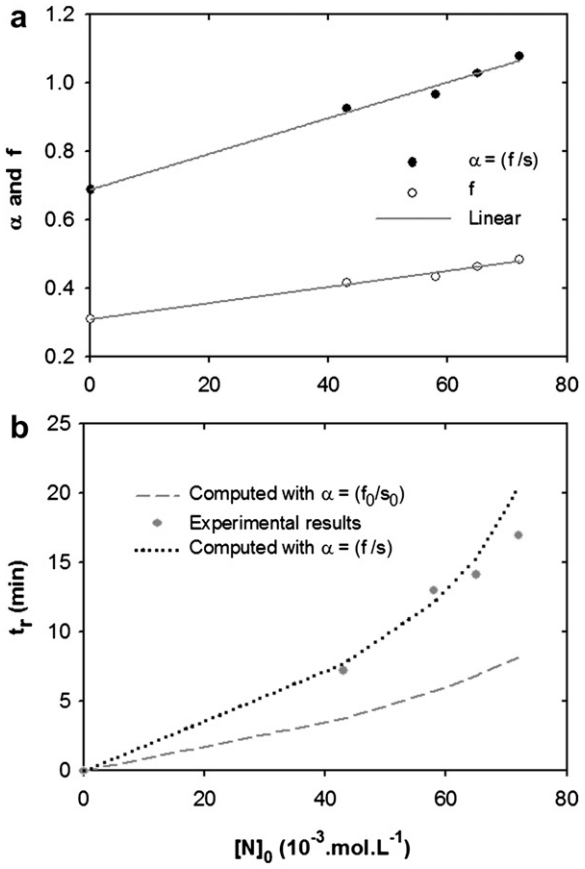

Fig. 2. Dependence of the initiator efficiency and scorch time on TEMPO concentration. $T = 160\ ^{\circ}C$. a) The linear lines are the best fit of experimental data according to Eq. (19) ($c_1 = 5.2$ and $\alpha_0 = 0.69$) and Eq. (20) ($c_2 = 2.34$ and $f_0 = 0.31$). Here '*a*' is Efficiency ratio and '*f*' is initiator efficiency. b) Comparison of computed and experimental values of the scorch time: Dashed line: $\alpha = f/s$ according to Eq. (19); Dotted line α = constant = f_0/s_0.

Moreover, Fig. 2b shows the TEMPO concentration dependence of t_r at $T = 160\ ^{\circ}C$. The experimental results do not agree well with the linear relation of t_r vs $[N]_0$; i.e., the experimental scorch time is higher than the predicted one from of Eq. (11) (with $f = f_0$, $s_0 = 0.21$ according to our previous work [7]). However, Fig. 2b shows that the predicted times t_r are in close agreement with experimental results using Eq. (11) with $\alpha = f/s$ as defined in Eq. (19).

4.2. Determination of k_{cc} using anisothermal DSC data

During crosslinking reaction the long chains of polymer chemically crosslink. Each covalent C–C bond formed between the

Table 1
Comparison between the experimental and calculated values of scorch time, efficiency of TEMPO and initiator.

$[N]_0$ (10^{-3} mol L^{-1})	r	$t_{r,exp}$ (min)	$t_{r,cal}$ (min)	$\alpha = f/s$	f	$[R_{cc}]$ mol m^{-3}	μ^a mol m^{-3}
0	0	0	0	0.689	0.31	11.1	10.1
43	1.2	7.2	7.7	0.926	0.417	5.07	5.6
58	1.6	13	12.2	0.966	0.435	2.96	4
65	1.8	14.1	15.3	1.029	0.463	1.97	2.6
72	2.0	16.9	20.4	1.078	0.485	1.02	1.6

NB: $[R_{cc}]$ is the total concentration of crosslinked bonds when the reaction is completed.
Initial concentration of DCP: $[DCP]_0 = 36 \times 10^{-3}$ mol L^{-1} and $T = 160\ ^{\circ}C$.
[a] Is retrieved from Ref. [7].

macromolecular chains of polymer releases a quantum of energy. One of the methods mostly used in the literature to determine enthalpy and kinetic parameters of this crosslinking reaction is thermal analysis by differential scanning calorimetry (DSC) at anisothermal mode [23]. The dynamic mode allowed us to estimate k_{cc} as a function of temperature. Indeed, reaction rate depends on time and temperature. Kissinger [24] was one of the first researchers who evaluated the kinetic parameters of a chemical reaction from the anisothermal DSC using peak temperature-heating rate data, with the following equation:

$$\ln\left(\dot{T}/T_{peak}^2\right) = \frac{E_{ac}}{R}\left(\frac{1}{T_{peak}}\right) - \ln\left(\frac{A_{0c}R}{E_{ac}}\right) \quad (21)$$

Where $\dot{T}$ is heating rate and R is the ideal gas constant. The kinetic parameter A_{0c} represents collision frequency factor and E_{ac} is activation energy for the bimolecular termination reaction (crosslinking reaction). Kissinger's method assumes that the maximum reaction rate occurs at peak temperatures (T_{peak}). Therefore, by plotting $\ln(\dot{T}/T_{peak}^2)$ versus $1/T_{peak}$ according to Eq. (21), E_{ac} can be then obtained from the slope of the corresponding straight line and A_{0c} corresponds to the ordinate at origin.

The anisothermal DSC scans of (PDMS/DCP/TEMPO) curing system at different amount of TEMPO ($r = 0$, 1.2, 1.6, 1.8 and 2) are shown in Fig. 3. Confirming our last original results with isothermal mode [7], these dynamic DSC kinetics allowed us to separate exothermic peak of C–C bonds creation from the other reactions like the homolytic decomposition of the initiator (DCP) and its addition on the polymer chains. Furthermore, the addition of TEMPO in the PDMS/DCP system results in a secondary exothermic peak, as shown in Fig. 3. This peak is assigned to C–C bonds creation. This hypothesis is validated by comparison of the rheological and DSC results in anisothermal mode for $r = 1.2$ as shown in Fig. 4. The end of the inhibition phase is observed by both techniques, i.e., strong variation of the complex shear modulus and evidence of a second exothermic peak. As a result, this peak temperature corresponds exactly to the network formation through the chemical crosslink reaction between PDMS polymer chains.

Experimentally, the peak temperature of the termination reaction shifts to higher temperatures with increasing the heating rate.

This is probably because the reaction takes place very rapidly at higher curing temperatures. More precisely, the dependence of $\ln(\dot{T}/T_{peak}^2)$ on $(1/T_{peak})$ is plotted and the linear variation of T_{peak} with the heating rate is observed to be in agreement with the Kissinger assumption based on the linear relation between peak temperature and heating rate. Consequently, E_{ac} and A_{0c} were

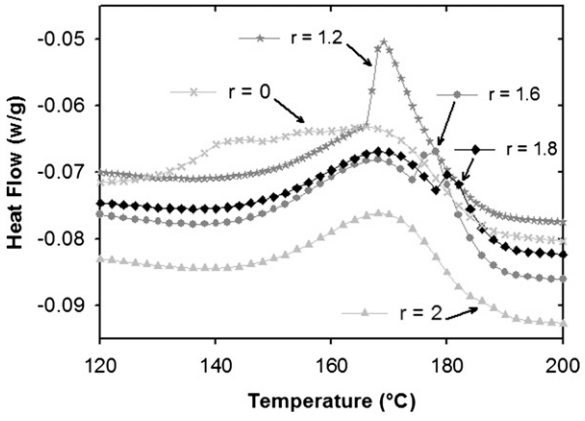

Fig. 3. DSC curves showing the total heat of crosslinking reaction obtained for various values of r at a heating rate of 2.5 °C min^{-1}. Where r = [TEMPO]/[DCP].

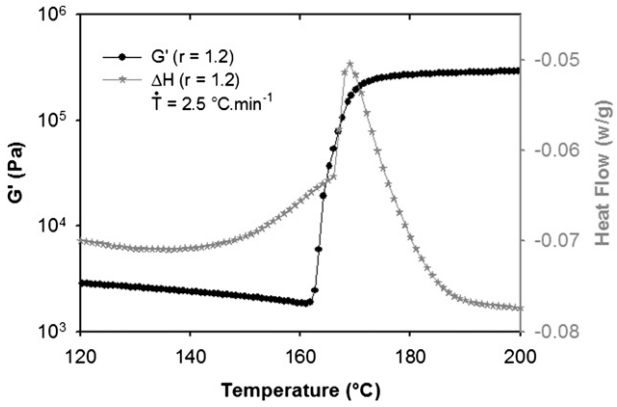

Fig. 4. Comparison of the variation of the storage modulus and enthalpy of the reaction ($r = 1.2$) under anisothermal condition = 2.5 °C min^{-1}.

calculated according to Eq. (21). The dependence of k_{cc} on the temperature can be expressed using the Arrhenius law:

$$k_{cc} = A_{0c}\exp\left(-E_{ac}/RT\right) \quad (22)$$

Where, $A_{0c} = 2.68 \times 10^{10}$ s^{-1} and $E_{ac} = 87{,}300$ J mol^{-1}.

4.3. Kinetics of chemical network growth

The influence of the experimental conditions ($[DCP]_0$, $[N]_0$, α and T) on the crosslinking reaction kinetics and network growth has been studied at the molecular scale according to this newly developed kinetic model. Note that in the following part Eqs. (19) and (20) were used to derive α and f respectively for use in Eqs. (14), (16) and (17).

According to Eq. (14) ($T = 160$ °C), the time-concentration variation of active PDMS carbon-centred radicals $[R_p^{\bullet}(t)]_{act}$ is plotted in Fig. 5a. Without TEMPO ($r = 0$), the initiation reaction occurs instantaneously and PDMS macro-radicals concentration increases to an optimal value followed by continuous decrease as the termination reaction is faster than initiation. In the presence of TEMPO, scorch time is highlighted and increases with increasing TEMPO concentration (i.e. the ratio r). From a modelling point of view, the active chains are created and instantaneously inactivated by TEMPO addition reaction during this inhibition phase. The residual concentration of DCP after the complete consumption of TEMPO can initiate other polymers chains so that the generation of $[R_p^{\bullet}(t)]_{act}$ can be observed as shown in Fig. 5a.

On the other hand, the optimal $[R_p^{\bullet}(t)]_{act}$ values for $t > t_r$ decrease with increasing the initial TEMPO concentration. Actually, this result was expected from our previous work [7]. We proved that the crosslinking delayed action in the presence of TEMPO is the result of trapped carbon-centred polymer radicals by nitroxides. Furthermore, TEMPO interacts with the macro-radicals from vinyl-PDMS during scorch phase to produce non-reactive species. Consequently, the bimolecular termination reaction is completely prevented ($[R_p^{\bullet}(t < t_r)]_{act} = 0$). Once TEMPO has completely reacted, the macro-radicals coupling (crosslink formation) starts in respect of the residual concentration $[R_p^{\bullet}(t > t_r)]_{act}$.

To show the key effect of TEMPO on the curing process, Fig. 5b compares the concentration variation of the crosslinking covalent bonds $[R_{cc}(t)]$ with the reaction time (according to Eq. (17) at $T = 160$ °C) for different initial concentrations of TEMPO. It can be clearly seen how TEMPO influences the scorch time, the crosslinking reaction rate and final concentration of crosslinking bonds ($[R_{cc}]$).

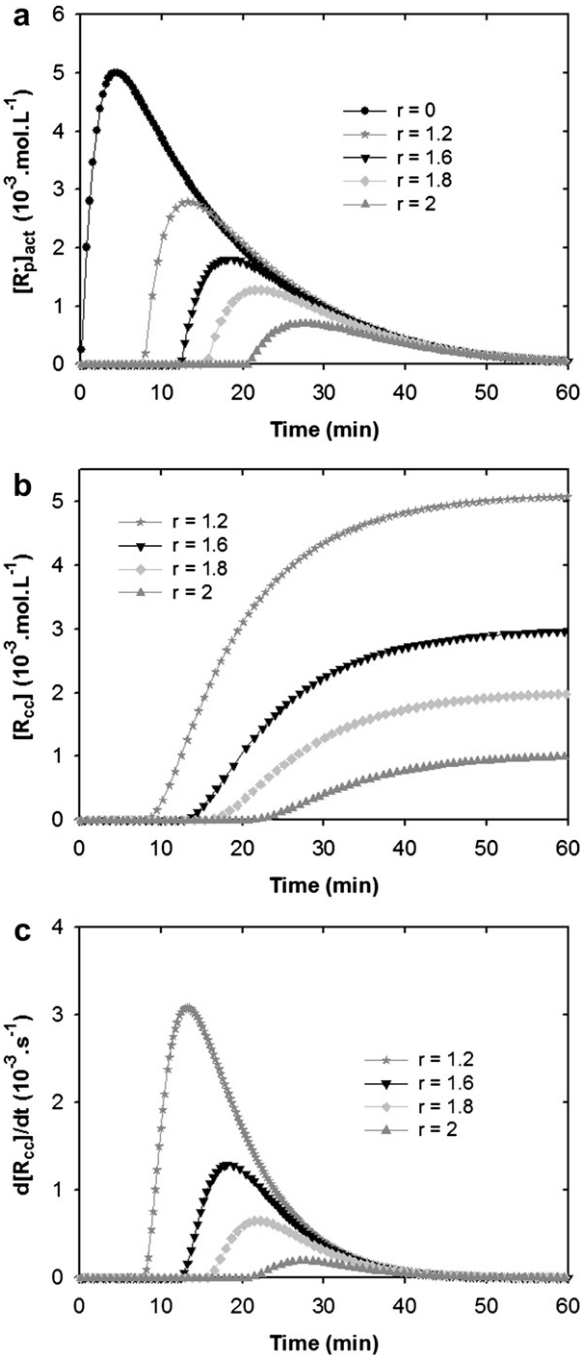

Fig. 5. Time dependence of PDMS crosslinking reaction for various values of r = [TEMPO]/[DCP]. T = 160 °C; $[DCP]_0 = 36 \times 10^{-3}$ mol L^{-1}. a) Variation of active carbon-centred radicals. b) Variation of crosslinked bonds concentration versus crosslinking time. c) Variation of crosslinking rate.

During the inhibition stage, TEMPO inactivate the primary PDMS macro-radicals and prevent the radical coupling $[R_{cc}(t < t_r)] = 0$. Therefore, if we accept that TEMPO is completely consumed during the scorch period and that the crosslinking reaction does not begin until TEMPO is totally consumed, the bimolecular termination reaction starts but it slows down due to lower concentration of initiator. Kinetically, the reduction in the concentration of active PDMS macro-radicals shown in Fig. 5a by TEMPO slows down the crosslinking rate ($d[R_{cc}(t)]/dt$) according to Eq. (5). According to these results, Fig. 5b demonstrated that TEMPO is a very powerful inhibitor for free-radical crosslinking of PDMS and that the crosslinking kinetics are entirely in agreement with the scheme in Fig. 1.

According to Fig. 5c, the rate of the crosslinking reaction $d[R_{cc}(t)]/dt$ predicted from Eq. (5) may be very low initially. These results explain the difference between kinetics of $[R_p^{\bullet}(t)]_{tot}$, $[R_p^{\bullet}(t)]_{act}$ and $[R_{cc}(t)]$ at the beginning of the macro-radicals coupling phase. It should be noted that $k_d = 2.3 \times 10^{-3}$ s^{-1} and $k_{cc} = 0.8$ L mol^{-1} s^{-1} at T = 160 °C, and the slow kinetic start of the chains recombination may be the result of the competition between the initiation and the bimolecular termination reactions. Thereafter, $d[R_{cc}(t)]/dt$ gradually increases to a maximum rate before decreasing with the decrease of $[R_p^{\bullet}(t)]_{act}$ at the end of crosslinking phase. Interestingly, we obtain the maximal values of $[R_{cc}] = 0.5 \times [R_p^{\bullet}]_{tot}$ at the end of the numerical computations (see Table 1), such as $[R_p^{\bullet}]_{tot} = 22.2\ 10^{-3}$ mol L^{-1} and $[R_{cc}] = 11.1\ 10^{-3}$ mol L^{-1} for $r = 0$ at T = 160 °C.

Furthermore, the comparison of the predicted final $[R_{cc}]$, i.e. when the reaction is completed, with our last results of μ (density of chemical crosslink bonds) [7] computed by using Pearson and Graessley model (presented in Table 1) shows a very satisfactory agreement which validates our kinetic hypothesis. On the other hand, the dependence of the computed final concentrations of crosslinking bonds $[R_{cc}]$ and total macro-radicals $[R_p^{\bullet}]_{tot}$ versus $[N]_0$ at T = 160 °C is shown in Fig. 6. It can be observed that optimal values of $[R_p^{\bullet}]_{tot}$ and $[R_{cc}]$ are linearly dependent on the initial TEMPO concentration. According to linear extrapolation of $[R_{cc}]$, the total amount of TEMPO necessary to totally prevent the crosslinking reaction ($[R_{cc}] = 0$) is then equal to 79×10^{-3} mol L^{-1}. Translating this value in terms of [TEMPO]/[DCP] ratio leads to r = 2.2. This result is in agreement with the value observed from rheological measurement r = 2.4 for which no crosslinking reaction was observed. In addition, these numerical results confirm our prediction using the DSC technique in the last experimental work [7].

Finally, it can be concluded from the variation of k_d and k_{cc} with temperature that our model is able to predict the variation of $[R_{cc}(t)]$ (including inhibition time) for any temperatures and any ratio. However, this temperature dependence is not plotted here for brevity and clarity. The temperature dependence will be checked in the next part on the variation the viscoelastic properties versus time for different values of r.

4.4. Rheo-kinetic modelling

The main objective of this work is to predict the changes in viscoelastic properties of PDMS during a free-radical crosslinking process controlled by the addition of TEMPO. We have established

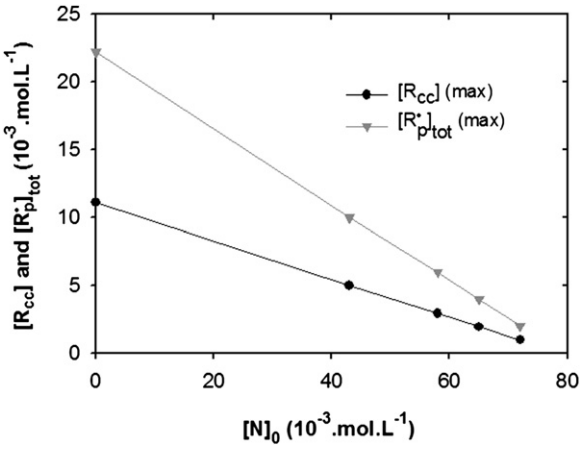

Fig. 6. Dependence of the final concentrations of crosslinking bonds, $[R_{cc}]$, and total macro-radicals, $[R_p^{\bullet}]_{tot}$ on the initial concentration of TEMPO at T = 160 °C.

in the previous part that the kinetic model is capable to predict peroxide decomposition [DCP(t)], active PDMS carbon-centred radicals $[R_p^{\bullet}(t)]_{act}$, and crosslink formation $[R_{cc}(t)]$. Then, rheo-kinetic modelling aims to predict the time variations of the complex shear modulus ($G'(t)_\omega$ and $G''(t)_\omega$). This can be achieved from the variation in crosslinking bonds formation $[R_{cc}(t)]$ derived from Eq. (17). However, at present we cannot theoretically predict the relationship between complex shear modulus and $[R_{cc}(t)]$; except when the reaction is completed (prediction of the equilibrium modulus). As far as we know, such kind of work for free-radical crosslinking process has never been reported in the literature from the standpoint of quantitative analysis. We solved this task by carrying out some experiments of crosslinking with different initial concentrations of DCP and TEMPO at $T = 160$ °C. Furthermore, combining Eq. (17) (kinetic model) and the experimental variation of complex shear modulus with the reaction time, we can experimentally express the variation of complex shear modulus versus radical coupling $[R_{cc}(t)]$ through a master curve.

From a numerical point of view, kinetic model was implemented through Matlab software. Fig. 7 plots the variation of the complex shear modulus versus the crosslinking bonds concentration $[R_{cc}(t)]$ for $r = 1.2$ at $T = 160$ °C, by using experimental variation of complex shear modulus and kinetic equation (17). We used this curve as a reference and the time dependence of complex shear modulus was predicted for any temperature and any initial DCP or TEMPO concentrations.

Fig. 8 shows the prediction of storage modulus $G'(t)_\omega$ for different [TEMPO]/[DCP] ratio at $T = 160$ °C. As expected, the addition of TEMPO results in the increase of the predicted scorch time t_r. In addition, all simulations exhibit a plateau after a long period of time which expresses the completion of crosslinking reaction. The frequency sweep experiment proved that this plateau is the equilibrium modulus G_e. However, it is clear that the time needed by the modulus to reach a plateau gets longer as TEMPO concentration increases. Furthermore, it can be seen that the rheo-kinetic model predicts a decrease in equilibrium storage modulus (G_e) as TEMPO input increases. As far as we know, such kind of results has never been reported in the literature from a quantitative viewpoint.

However, Fig. 8 shows that the model slightly overestimates the equilibrium storage modulus for $r = 1.8$ and 2. This result can be explained by the fact that the Rheo-kinetic model overestimates the effect of physicals entanglements for lower equilibrium storage modulus. Actually the time variation of complex shear modulus for

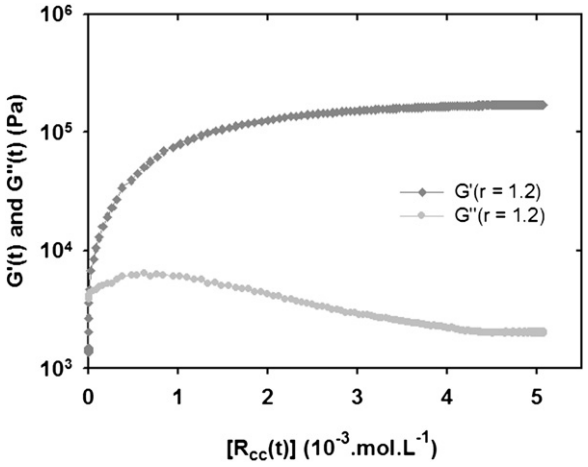

Fig. 7. Variation of the complex shear modulus versus the effective concentration of crosslinking bonds [R_{cc}] at $T = 160$ °C. This curve was used as reference for modelling developments.

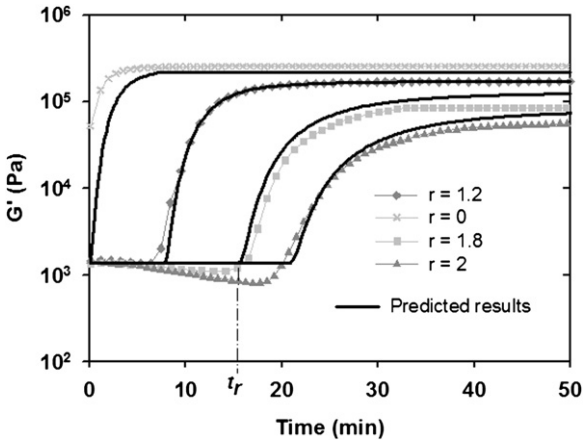

Fig. 8. Modelling of the time variations of storage modulus for different ratios: $r = 0$, 1.2, 1.8, 2 ($T = 160$ °C). Solid curves are obtained from simulations, while patterned lines are drawn from experimental data.

$r = 1.2$ was used as reference curve. So the rheological model includes the trapped physical entanglements. Nevertheless, the probability of such trapping is expected to decrease with decreasing the crosslinking density; whereas the model takes into account a constant probability whatever the final crosslinking density. Moreover, Fig. 8 shows a slowly decrease in the experimental storage modulus at the earlier stage of reaction. This phenomenon is

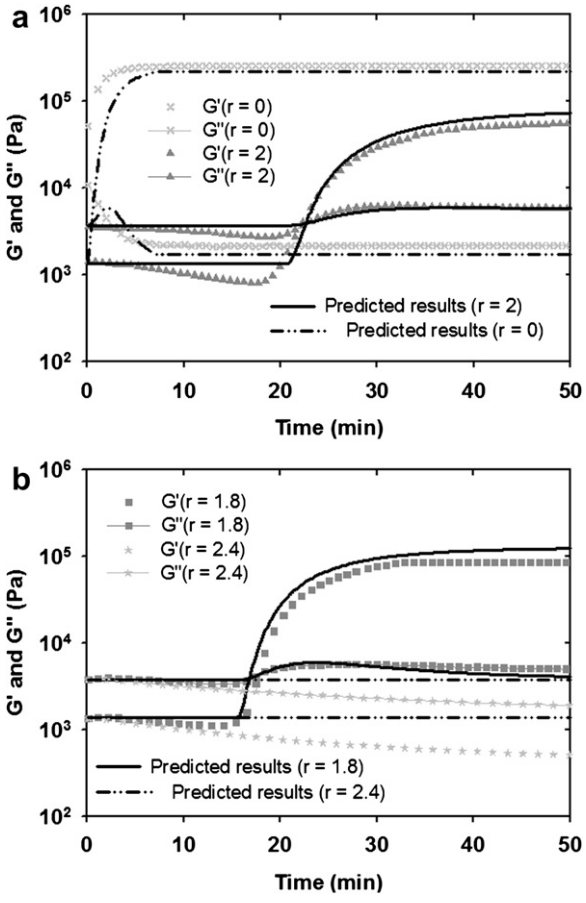

Fig. 9. Modelling of the time variation of the complex shear modulus for different [TEMPO]/[DCP] ratios ($T = 160$ °C Solid curves are obtained from simulations, while patterned lines are drawn from experimental data. a) $r = 0$ and $r = 2.0$. b) $r = 1.8$ and $r = 2.4$.

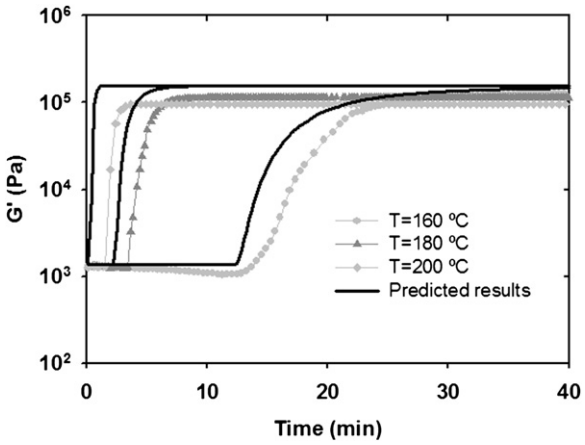

Fig. 10. Modelling of the time variation of the storage modulus for different temperatures at r = [TEMPO]/[DCP] = 1.6. Solid curves are obtained from simulations, while patterned lines are drawn from experimental data.

clearly shown for $r = 2$. This significant decrease in complex modulus may be attributed to PDMS degradation in the presence of TEMPO nitroxide. This behaviour cannot be predicted here because the complex degradation mechanism (detailed in our previous work [7]) was not investigated in the present kinetic model.

Comparison of the predicted storage and loss modulus with rheometer data for different [TEMPO]/[DCP] ratios at $T = 160$ °C is shown in Fig. 9a and b. From a qualitative point of view, the viscoelastic variation of $G'(t)_\omega$ and $G''(t)_\omega$ was remarkably predicted by the rheo-kinetic model. Interestingly, Fig. 9b shows that at higher amount of TEMPO ($r = 2.4$), the rheo-kinetic model predicted that the crosslinking reaction was totally prevented.

Finally, Fig. 10 shows that the rheo-kinetic model predicts well the variation of storage modulus versus time at different temperatures ($T = 160$, 180, and 200 °C) for $r = 1.6$. As experimentally observed, the rheo-kinetic model predicts that the scorch time decreases with the increase in temperature. For example, the model predicts that t_r shifted from 12.2 min at 160 °C to 2.2 min at 180 °C and crosslinking becomes 'instantaneous' at 200 °C. Finally, as expected from our hypothesis, the model predicts that the equilibrium modulus does not depend on the temperature. This behaviour is not observed for the experimental variation due to side reactions which can occur at higher temperatures ($T > 170$ °C) according to Mskani et al. [15].

5. Conclusion

In this study, a new rheological modelling method was developed to predict the variation of complex shear modulus for PDMS network formation under free-radical crosslinking reaction controlled by TEMPO. This new method is based on the relationship between the kinetics of macro-radicals coupling [$R_{cc}(t)$] derived from a fundamental kinetic model and the viscoelastic variation of complex shear modulus ($G'(t)_\omega$ and $G''(t)_\omega$). Owing to the complexity of crosslinking chemistry, a simplified reactions scheme was used to establish the fundamental kinetic model.

First of all, a kinetic model was derived in order to predict the crosslinking process including decomposition of peroxide [DCP(t)], active PDMS carbon-centred radicals $[R_p^\bullet(t)]_{act}$ creation, inhibition reaction time t_r and the crosslinking bonds formation [$R_{cc}(t)$]. The influence of formulation conditions such as ($[DCP]_0$, [TEMPO]/[DCP] and Temperature) on the crosslinking reaction kinetics and network growth, has been studied at the molecular scale according to this kinetic model. It was observed that the addition of TEMPO nitroxide can boost the initiator efficiency. On the other hand, the Kissinger DSC method was used to calculate the activation energy E_{ac} (87,300 J mol^{-1}) and the collision frequency factor A_{0c} (2.68×10^{10} s^{-1}) for the bimolecular termination reaction rate k_{cc}.

Finally, the rheological modelling shows that this new method precisely predicts the time variation of the complex shear modulus at any temperature and [TEMPO]/[DCP] ratio. Although this modelling has been developed for PDMS rubber, it can easily be extended to any rubber crosslinking via radical chemistry in the presence of nitroxide.

References

[1] Yuxi J, Sheng S, Shuxia X, Lili L, Guoqun Z. Polymer 2002;43:7515–20.
[2] Blaz L, Matjaz K. Polym Eng Sci 2008;49:60–72.
[3] Yuxi J, Sheng S, Lili L, Yue M, Lijia A. Acta Materialia 2004;52:4153–9.
[4] Baquey G, Moine L, Degueil-Castaing M, Lartigue JC, Maillard B. Macromolecules 2005;38(23):9571–83.
[5] Dorn M. Adv Polym Technol 1985;5:87–91.
[6] Chaudhary BI, Chopin L, Klier J. J Polym Sci 2007;47:50–61.
[7] Mani S, Cassagnau P, Bousmina M, Chaumont P. Macromolecules 2009;42:8460–7.
[8] Langley NR. Macromolecules 1968;1:348–52.
[9] Dossin LM, Graessley WW. Macromolecules 1979;12:123–30.
[10] Robert PM. EP 0,837,080, A1; 1997.
[11] Esseghir M, Chaudhary BI, Cogen, Jeffrey M, Klier J, Jow J, et al. US Patent 7, 465, 769 B2; 2008.
[12] Ciullo PA, Hewitt N. "The rubber formulary". New York; 1999.
[13] Dluzneski PR. Rubber Chem Technol 2001;74:451–92.
[14] Kurdikar DL, Peppas NA. Macromolecules 1994;27:4084–92.
[15] Msakni A, Chaumont P, Cassagnau P. Rheol Acta 2007;46:933–43.
[16] Flat JJ. Private communication. Internal report from Arkema Company; 2004.
[17] Russell KE. Prog Polym Sci 2002;27:1007–38.
[18] Zhou W, Zhu S. Macromolecules 1998;31:4335–41.
[19] Berzin F, Vergnes B, Dufosse P, Delamare L. Polym Eng Sci 2000;40(2):344–56.
[20] Bamford CH, Tipper CFH. Free-radical polymerisation-comprehensive chemical kinetics, vol. 14A. New York: Elsevier; 1976. p. 7 [Chapter 1]. .
[21] Han CD, Lee DS. J Appl Polym Sci 1987;34:793–813.
[22] Zhang M, Ray WH. J Appl Polym Sci 2002;86:1630–62.
[23] Yousefi A, Lafleur PG. Polym Comp 1997;18(2):157–68.
[24] Kissinger HE. Anal Chem 1957;29:1702–6.